Molecular Recognition of 1-(2-Octadecyloxycarbonylethyl)cytosine Monolayers to Guanosine at the Air−Water Interface Investigated by Infrared Reflection−Absorption Spectroscopy

Wangen Miao, Xuezhong Du,* and Yingqiu Liang*

Key Laboratory of Mesoscopic Chemistry, Ministry of Education, Nanjing University, Nanjing 210093, People's Republic of China

Received: June 30, 2003; In Final Form: October 10, 2003

Molecular recognition of 1-(2-octadecyloxycarbonylethyl)cytosine monolayers at the air−water interface to complementary guanosine bases in the subphase has been studied using infrared reflection−absorption spectroscopy. It is the first time that the exact sites in the cytosine rings involved in the triple hydrogen-bonding interaction between complementary base pairs cytosine and guanosine are distinguished with the in situ technique. It is shown that the cytosine rings undergo a flat-on orientation before molecular recognition to an end-on one after molecular recognition and that the alkyl chains are more tilted after molecular recognition. Further simulation calculation shows that the tilt angle of the alkyl chains in the monolayers undergoes a change from 20° with respect to the film normal before molecular recognition to 30° after molecular recognition, which indicates that the chain orientation is strongly influenced by the recognition interaction between the cytosine moieties in the monolayers and the complementary guanosine bases in the subphase.

Introduction

Molecular recognition by means of multiple hydrogen bonds is of great importance in biological functions because the mutual recognition of Watson−Crick complementary bases in nucleic acids is the basis of their stable double-helix structure and the most efficient mechanism of accumulating, storing, and evolving genetic information.[1] Some derivatives of nucleotides, including nucleolipid amphiphiles, have been found to possess anticancer and antivirus properties.[2,3] Analysis and mimicry of the molecular recognition processes not only will lead to a better understanding of biomembrane functions and processes but also can be helpful in the development of the novel medicine and biological sensors.[2,4]

DNA-linked nucleobases are well known to undergo molecular recognition through both hydrogen bonds and $\pi-\pi$ stacking for nucleic acid stabilization, while isolated nucleosides only show simple stacking in bulk water due to the strongly competitive binding of surrounding water molecules.[5−7] To mimic the molecular recognition properties of complementary nucleobases in aqueous systems by way of chemistry, several mimetic systems, such as micelles,[8−10] vesicles,[11−13] and monolayers at the air−water interface,[14−28] have been developed in the past decades. A pioneering work on the base-pair mimic at the air−water interface was described by Kitano et al. by use of surface pressure (π)−area (A) isotherms.[29] The organized nucleolipid monolayers at the air−water interface might act as single nucleic acid strands, due to the hydrophobic interaction between the corresponding alkyl chains, to recognize complementary bases in the subphase. Thereafter, much work about molecular recognition at the air−water interface between nucleolipids and their complementary bases dissolved in the subphase was reported.[14−28] To obtain information on molecular recognition at the molecular level, the Langmuir−Blodgett (LB) technique has been used to study molecular recognition between nucleolipids and their complementary bases dissolved in the subphase by means of UV, FTIR, and surface-enhanced Raman scattering (SERS) spectroscopy.[21−27] However, the information obtained was indirect due to the water-free environment and substrate effect in the LB films. To have a full understanding of the mimetic molecular recognition in aqueous environment, which is close to that of DNA and RNA in biological systems, a direct, in situ characterization method is necessary for studying molecular recognition at the molecular level.

Infrared reflection−absorption spectroscopy (IRRAS) has been a leading structural method for the in situ characterization of Langmuir monolayers at the air−water interface at the molecular level[30−41] since the early works by Dluhy and coworkers.[42] The IRRAS technique provides information not only on molecular interaction between headgroups and substances dissolved in the subphase but also on orientation of alkyl chains.[32f,h,40] However, few studies so far have been concerned with the characterization of the mimetic molecular recognition via hydrogen bonds.[20,28] In this paper, molecular recognition of the monolayers of nucleolipid 1-(2-octadecyloxycarbonylethyl)cytosine at the air−water interface to complementary guanosine bases in the subphase has been investigated using the IRRAS technique. The chain orientation prior to and after molecular recognition is quantitatively calculated by use of theoretical simulation. The molecular recognition gives rise to a change in orientation of hydrophilic headgroups and hydrophobic chains.

Experimental Section

Materials. The synthesis of the nucleolipid amphiphile, 1-(2-octadecyloxycarbonylethyl)cytosine, was recently described in detail,[27] and its chemical structure is illustrated in Figure 1a. Guanosine was purchased from Sigma and used as received (its chemical structure is shown in Figure 1b). H_2O used for the subphase was deionized and doubly distilled. D_2O (99.95% isotopic enrichment) was obtained from Beijing Chemicals Company.

IRRAS Spectral Measurements. IRRAS measurements of nucleolipid monolayers at the air−water interface were per-

* To whom correspondence should be addressed. Fax: 86-25-3317761. E-mail: yqliang@nju.edu.cn (Y.L.); duxz2000@yahoo.com (X.D.).

10.1021/jp035880t CCC: $25.00
Published on Web 11/15/2003

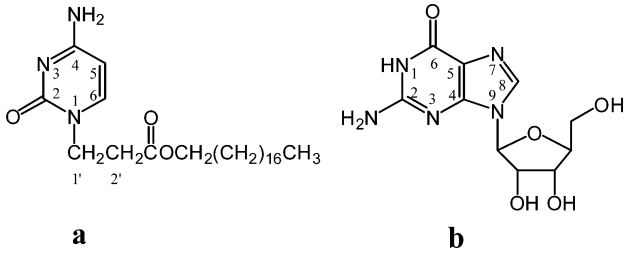

Figure 1. Chemical structures of (a) nucleolipid 1-(2-octadecyloxycarbonylethyl)cytosine and (b) complementary base guanosine.

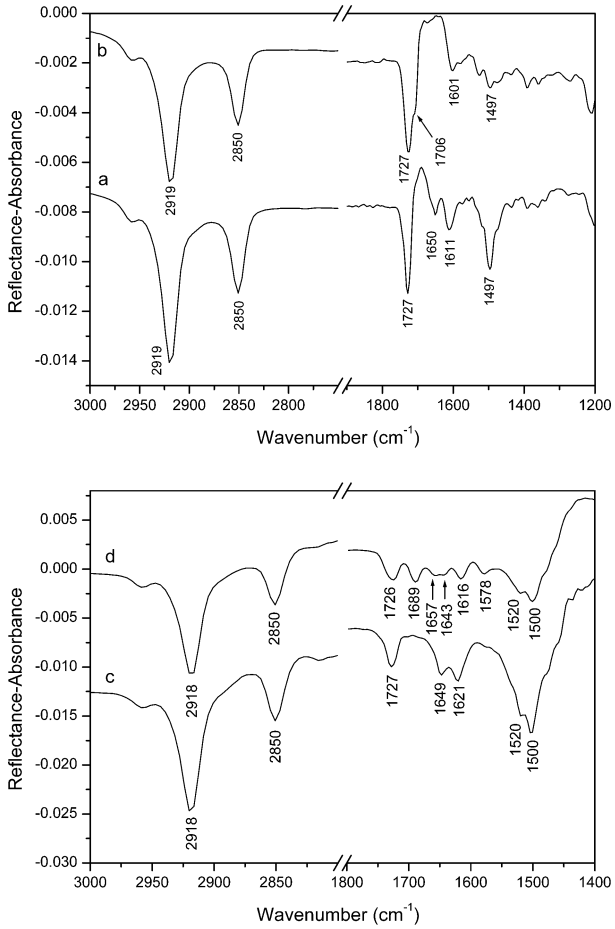

Figure 2. IRRAS spectra of 1-(2-octadecyloxycarbonylethyl)cytosine monolayers on (a) H_2O, (b) H_2O guanosine solution (top), (c) D_2O, and (d) D_2O guanosine solution (bottom) at the 30° angle of incidence for p polarization (π = 20 mN/m).

formed on an Equinox 55 FTIR spectrometer equipped with a Bruker XA-511 external reflection attachment with a shuttle Langmuir trough using a MCT detector (Bruker, Germany). The rate of the shuttle movement is 10 mm/min. A faster speed would disturb the Langmuir monolayers, while a slower speed would prolong the experimental time. The surface pressures were always monitored during IRRAS scans. The temperature was set to 293 K. The spectra were recorded with a resolution of 8 cm^{-1} by coaddition of 2048 scans, and a relatively high signal−noise ratio could be obtained by carefully controlling the experimental conditions. The external reflection−absorption spectra of H_2O or D_2O and 1 mM H_2O or D_2O guanosine solution were used as references for the spectra before and after molecular recognition, respectively. All of the infrared spectra were used without any smoothing. The film-forming molecules were spread from the chloroform solution on an area of about 120 $Å^2$ per molecule. After the chloroform was evaporated, the

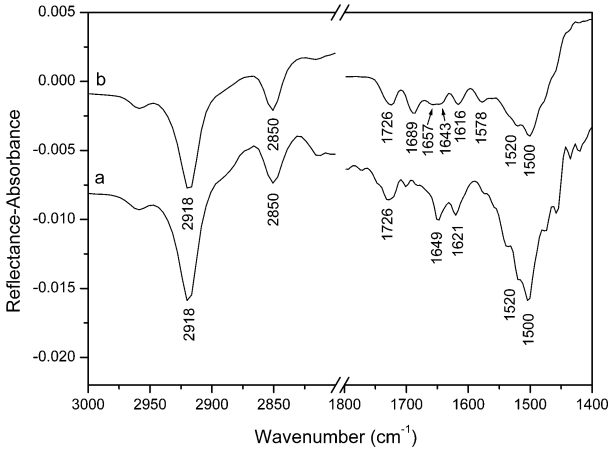

Figure 3. IRRAS spectra of 1-(2-octadecyloxycarbonylethyl)cytosine monolayers on (a) D_2O and (b) D_2O−guanosine solution subphases (π = 20 mN/m) at the 30° angle of incidence for s polarization.

measurement system was closed for the equilibrium of humidity and the relaxation of the monolayers for 4 h prior to compression. The monolayers were then compressed discontinuously with an initial step width of 0.8 $Å^2$ per molecule to a set value of surface pressure (π = 20 mN/m in this paper). Twenty minutes was allowed for the relaxation of the films before scanning procedures. As shown in our recent paper,[27] the $\pi-A$ isotherms suggest that the Langmuir monolayers both on pure water and in guanosine solution undergo a transition from a liquid-condensed phase to a solid phase around 15 mN/m. The monolayers at the pressure π = 20 mN/m are stable for the investigation of the molecular recognition at the air−water interface. In the spectral scanning procedures, the surface pressure is kept at 20 mN/m by adjusting the moving barriers forward or backward slightly. There are two advantages for the use of a shuttle system in the experimental setup;[32h] one is a good water vapor match between reference and sample, and the other is that the spectra of s- and p-polarized radiation could be acquired from the same monolayer by switching the polarizer to s or p polarization.

Results and Discussion

Molecular Recognition of 1-(2-Octadecyloxycarbonylethyl)cytosine Monolayers to Guanosine at the Air−Water Interface. Figure 2 (top) shows the IRRAS spectra of 1-(2-octadecyloxycarbonylethyl)cytosine monolayers at the air−water interface on H_2O (part a) and its guanosine solution (part b) subphases (π = 20 mN/m) at the 30° incident angle for p polarization. Both the scissoring vibrational bands of H_2O and the vibrational bands of the C═O, C═C, C═N stretching, and NH_2 bending modes relevant to nucleic acid bases appear in the spectral region 1800−1400 cm^{-1}. It is hard to attribute the absorption bands and to distinguish the spectral changes in this region for the monolayers on H_2O and its guanosine solution subphases. That means that it is difficult to assign the characteristic bands unambiguously and to obtain definite information on interaction between cytosine moieties in the monolayers and complementary guanosine bases in the subphase. When the subphase H_2O is replaced by D_2O, the in-plane bending band of D_2O is shifted to the region 1300−1150 cm^{-1} so that the characteristic absorption bands due to the C═O, C═C, C═N stretching, and NH_2 bending modes will be easily observed.

Figure 2 (bottom) shows the IRRAS spectra of 1-(2-octadecyloxycarbonylethyl)cytosine monolayers on D_2O

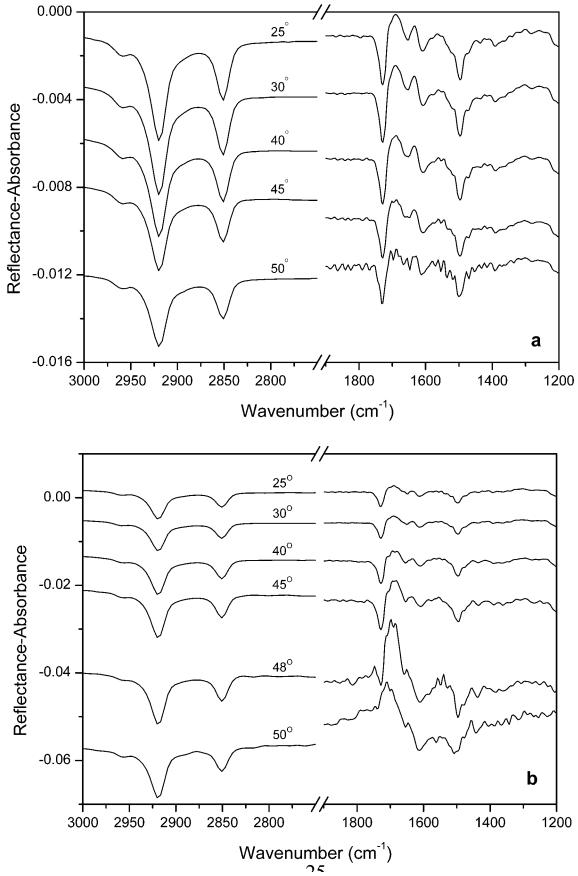

Figure 4. IRRAS spectra of 1-(2-octadecyloxycarbonylethyl)cytosine monolayers on the H_2O subphase at different incident angles ($\pi = 20$ mN/m): (a) s polarization, (b) p polarization.

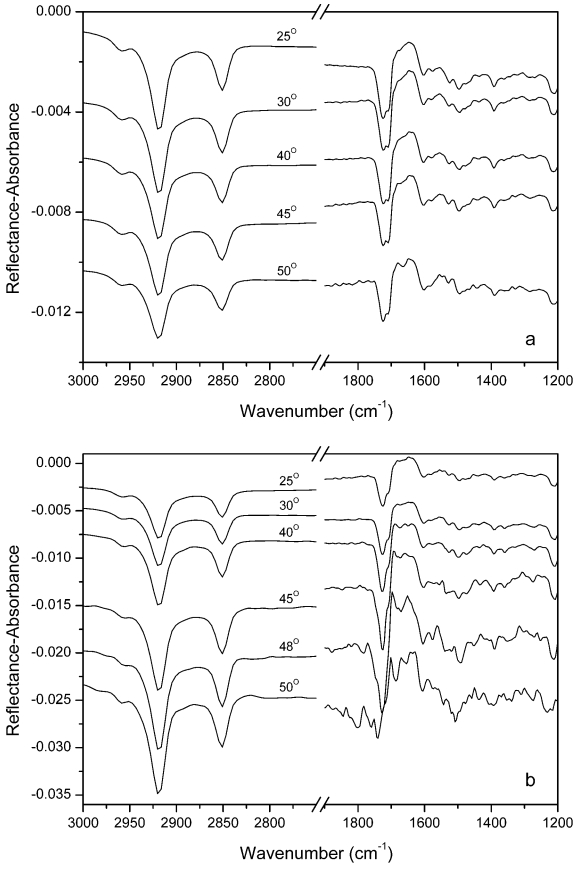

Figure 5. IRRAS spectra of 1-(2-octadecyloxycarbonylethyl)cytosine monolayers on 1 mM H_2O guanosine solution subphase at different incident angles ($\pi = 20$ mN/m): (a) s polarization, (b) p polarization.

(part c) and its guanosine solution (part d) subphases ($\pi = 20$ mN/m) at the 30° incident angle for p polarization. The two strong bands near 2918 and 2850 cm^{-1} are due to the $\upsilon_a(CH_2)$ and $\upsilon_s(CH_2)$ vibrations of long hydrocarbon chains, respectively. It is well known that the $\upsilon_a(CH_2)$ and $\upsilon_s(CH_2)$ frequencies are sensitive to the conformational order of the hydrocarbon chains. When the chains are highly ordered (all-trans conformation), the two bands appear at 2918 and 2850 cm^{-1}, but if conformational disorder is included in the alkyl chains, they shift upward to 2924 and 2856 cm^{-1}, respectively, depending upon the content of gauche conformers.[43−45] The $\upsilon_a(CH_2)$ and $\upsilon_s(CH_2)$ frequencies at 2918 and 2850 cm^{-1} suggest that the alkyl chains are highly ordered with almost all-trans conformations. For the monolayer on the D_2O subphase (Figure 2c), the single band at 1727 cm^{-1} is assigned to the C═O stretching vibration (υ(C═O)) in the ester groups, while the band at 1649 cm^{-1} is ascribed to the mixed modes of the C(2)═O stretching (υ(C(2)═O))[46,47] and NH_2 bending ($\delta(NH_2)$) vibrations in the cytosine moieties.[46,47] The band at 1621 cm^{-1} is due to the coupled stretching vibrations of the N(3)═C(4) and C(5)═C(6) bonds in the cytosine rings,[46,47] and the bands at 1520 and 1500 cm^{-1} are attributed to the coupled cytosine ring vibrations.[46,47] For the monolayer on the D_2O−guanosine solution subphase (Figure 2d), the changes in characteristic vibrational bands are obviously observed. Two new bands appear at about 1689 and 1578 cm^{-1}, which are attributed to the C(6)═O stretching vibration[47,48] and the coupled modes of C(2)═N(3) and C(8)═N(7) stretching vibrations[47,48] in the guanine moieties in the subphase, respectively. Two new peaks near 1657 and 1643 cm^{-1} in Figure 2d are generated from the original mixed band at 1649 cm^{-1} of the C(2)═O stretching and NH_2 bending modes in Figure 2c due to the frequency shift, which suggests the formation of hydrogen bonds between the cytosine moieties in the monolayers and the guanosine in the subphase. It is known that the hydrogen-bonding interaction would give rise to a lower wavenumber shift of the stretching mode and a higher wavenumber shift of the bending mode.[49] So the band at 1657 cm^{-1} is attributed to the NH_2 bending vibration, and the band at 1643 cm^{-1} is assigned to the C(2)═O stretching mode in the cytosine rings. The coupled band due to the N(3)═C(4) and C(5)═C(6) stretching vibrations in the cytosine rings also takes a shift from 1621 to 1616 cm^{-1}, which indicates that the atoms of N(3) in the cytosine rings are also involved in the hydrogen-bonding interaction between the monolayers and the complementary bases in the subphase. All of these spectral changes suggest the occurrence of molecular recognition by means of triple hydrogen bonds in the sites of the C(2)═O, N(3), and NH_2 in the cytosine rings to the complementary guanosine bases. It is clearly seen that the IRRAS spectra not only provide powerful evidence for molecular recognition between the nucleolipid monolayers at the air−water interface and the complementary bases in the subphase but also confirm the exact sites of the triple-hydrogen-bonding interaction. This result is in good agreement with the conventional concept, in which triple hydrogen bonds are formed between the Watson−Crick complementary bases pairs, cytosine and guanine pairs in DNA and RNA.

It is well known that the electric field vector of s polarization, E_s, is always parallel to the water surface, so the IRRAS spectra for s polarization can be directly used to perform qualitative analysis of the functional group orientation. When the transition dipole moment of a functional group is parallel to E_s, the band

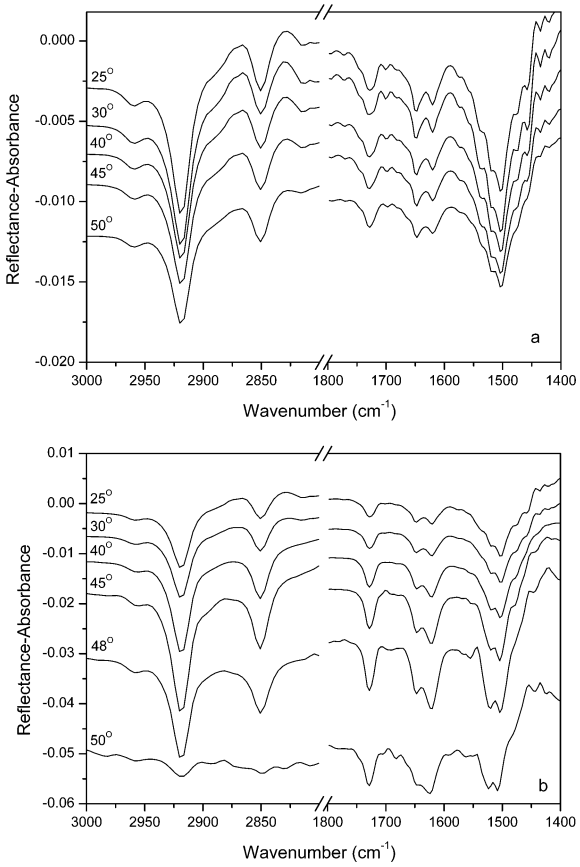

Figure 6. IRRAS spectra of 1-(2-octadecyloxycarbonylethyl)cytosine monolayers on the D_2O subphase at different incident angles ($\pi = 20$ mN/m): (a) s polarization, (b) p polarization.

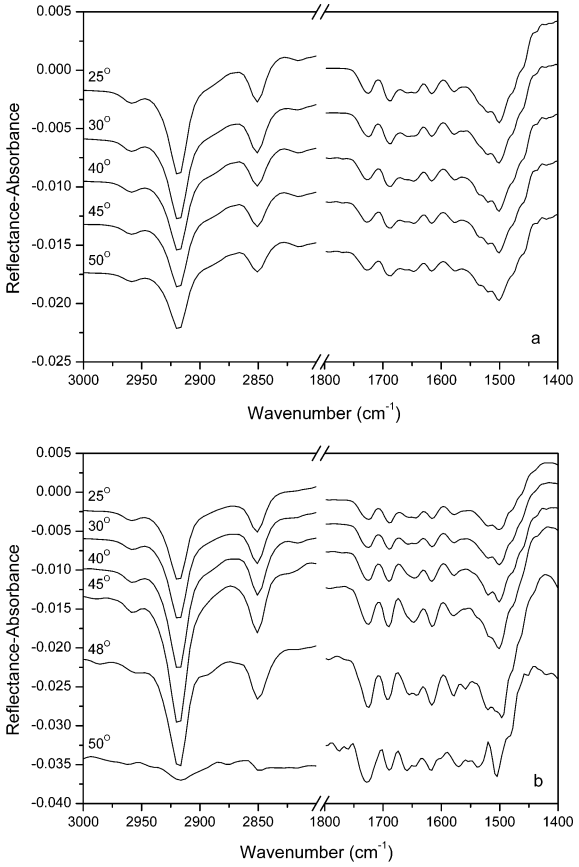

Figure 7. IRRAS spectra of 1-(2-octadecyloxycarbonylethyl)cytosine monolayers on 1 mM D_2O−guanosine solution subphase at different incident angles ($\pi = 20$ mN/m): (a) s polarization, (b) p polarization.

intensity will be maximal. When the transition dipole moment is perpendicular to E_s, the band intensity will be undoubtedly minimal.

Figure 3 shows the IRRAS spectra of 1-(2-octadecyloxycarbonylethyl)cytosine monolayers on D_2O and its guanosine solution subphases ($\pi = 20$ mN/m) at the incident angle 30° for s polarization. It can be seen that the intensities of the bands at 1649, 1621, 1520, and 1500 cm^{-1} due to the skeletal vibrations of cytosine rings are greatly reduced after molecular recognition. Since the transition dipole moments of these skeletal vibrations are parallel to the planes of the cytosine rings, the reduction in the band intensities suggests that the cytosine planes undergo a change from a preferred flat-on orientation before molecular recognition to a favorable end-on one after molecular recognition. At the same time, the reduction in the $\upsilon_a(CH_2)$ and $\upsilon_s(CH_2)$ band intensities to some degree also indicates that the alkyl chains become more tilted with respect to the film normal after molecular recognition because the transition dipole moments of the $\upsilon_a(CH_2)$ and $\upsilon_s(CH_2)$ modes are perpendicular to the axes of the alkyl chains.

Both the IRRAS studies of the monolayers at the air−water interface and the transmission FTIR studies of the corresponding LB films[27] provide evidence for the formation of hydrogen bonds between the cytosine moieties in the monolayers and the complementary guanosine bases and information on cytosine ring orientation from a flat-on geometry before molecular recognition to an end-on one after molecular recognition. That means that the LB transfer technique basically maintains the orientation of molecules in the monolayers at the air−water interface. However, the exact sites in the cytosine rings in the monolayers involved in the triple hydrogen-bonding interaction with complementary guanosine bases are clearly observed by the IRRAS technique.

Calculation Simulation of Chain Orientation. Figures 4 and 5 show the IRRAS spectra of 1-(2-octadecyloxycarbonylethyl)cytosine monolayers on H_2O and its guanosine solution subphases at different angles of incidence for s and p polarization, respectively, and Figures 6 and 7 show the IRRAS spectra of the monolayers on D_2O and its guanosine solution subphases at different angles of incidence for s and p polarization, respectively. It is found that the $\upsilon_a(CH_2)$ and $\upsilon_s(CH_2)$ bands for D_2O-based subphases (Figures 6 and 7) are nearly twice as strong as the respective H_2O-based bands (Figures 4 and 5). It could be seen that for s polarization (part a of Figures 4−7), the intensities of the negatively oriented bands decrease along with increasing angle of incidence, while for p polarization (part b of Figures 4−7), the intensities increase and reach a maximum around the given incident angle. On H_2O and its guanosine solution subphases (part b of Figures 4 and 5), the maximum values of the $\upsilon_a(CH_2)$ and $\upsilon_s(CH_2)$ band intensities appear around the 50° incident angle, and on D_2O and its guanosine solution subphases (part b of Figures 6 and 7), the maximum appears around 45°. The differences between them are owing to the difference in complex refractive index of subphase, $\tilde{n}_{H_2O} = 1.402 + 0.0157i$, $\tilde{n}_{D_2O} = 1.239 + 0.0022i$.[56] The Brewster angles, determined by calculating the tangents of the real part of the subphase refractive index, are 54.5 and 54.2° for H_2O and 51.1 and 50.7° for the D_2O subphases in the spectral region of the $\upsilon_a(CH_2)$ and $\upsilon_s(CH_2)$ modes, respectively.[32h] As shown previously, bands for p-polarization radiation reverse their signs at the Brewster angle.[30,32h,40,42] In the spectra at the 50° incident angle, the $\upsilon_a(CH_2)$ and $\upsilon_s(CH_2)$ band intensities are considerably

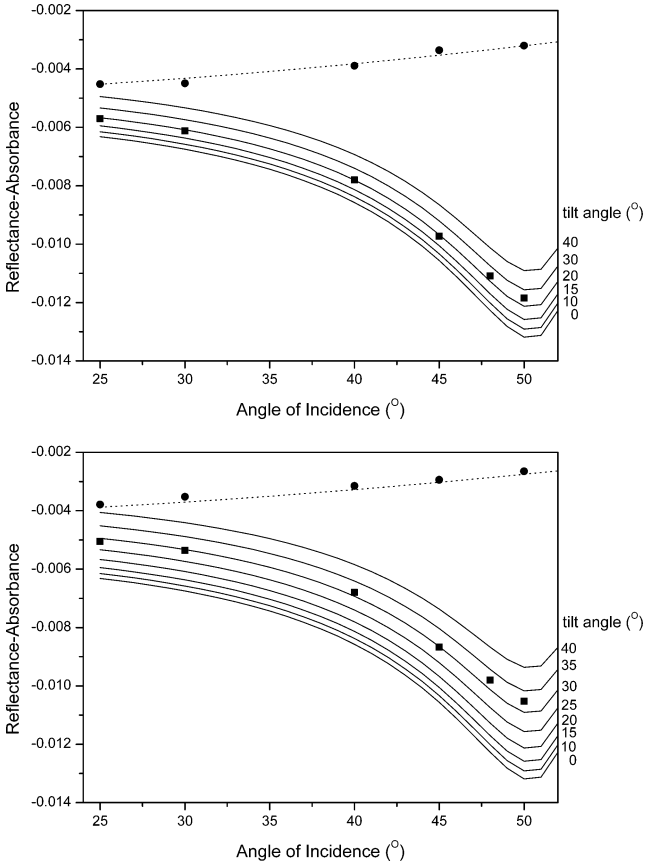

Figure 8. Comparison of the simulated (dotted and solid lines for s and p polarization, respectively) and measured $\upsilon_a(CH_2)$ intensities for s polarization (●) and p polarization (■) on H_2O (top) and its guanosine solution (bottom) subphases, respectively. Tilt angle $\theta = 20°$ is the best fit for the H_2O subphase, and $\theta = 30°$ is the best fit for the H_2O−guanosine solution subphase. The surface film parameters for simulation are $k_{max} = 0.50$, $\Gamma = 0.013$, $\alpha = 90°$, $L = 2.78$ nm, and $d = 2.63$ and 2.41 nm for H_2O and its guanosine solution subphases, respectively.

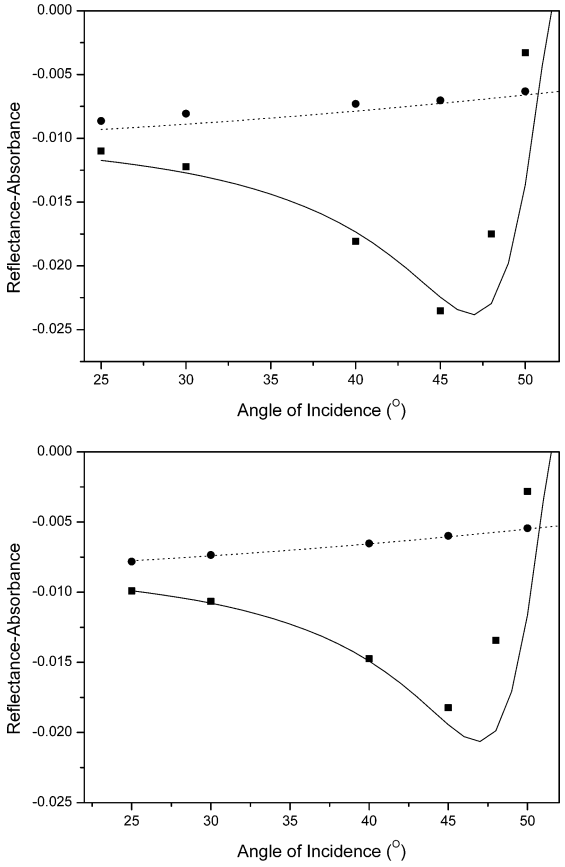

Figure 9. Comparison of the simulated (dotted and solid lines for s and p polarization, respectively) and measured $\upsilon_a(CH_2)$ intensities for s polarization (●) and p polarization (■) on D_2O (top) and its guanosine solution (bottom) subphases. Tilt angle $\theta = 20°$ for the D_2O subphase, and $\theta = 30°$ for the D_2O−guanosine solution subphase. The surface film parameters for simulation are $k_{max} = 0.50$, $\Gamma = 0.013$, $\alpha = 90°$, $L = 2.78$ nm, and $d = 2.63$ and 2.41 nm for D_2O and its guanosine solution subphases, respectively.

greater on H_2O (part b of Figures 4 and 5) than on D_2O for p-polarization radiation to the extent that the $\upsilon_s(CH_2)$ bands for p-polarization radiation vanish on the D_2O subphase. These observations are consistent with the difference between the Brewster angle and the incident angle 50° for each phase. As shown later, deviations from ideal polarization characteristics, especially in p-polarized spectra, cause deviations from the expected variations in the intensities with the incident angle.

It is well known that the IRRAS data are defined as plots of reflectance−absorbance (RA) vs wavenumber. RA is defined as $-\log(R/R_0)$, where R and R_0 are the reflectivities of the film-covered and film-free surfaces, respectively. Three different theoretical optical models have been employed to simulate RA by Schopper,[50] Kuzmin and Michailov,[51] and Yamamato and Ishida,[52] and similar results were obtained from the three formulations upon computer simulation. Herein we use Kuzmin and Michailov's model, which was first applied by Gericke et al.[31b,32f,h,40,42b,53−55] in detail to describe IRRAS band intensities. Among the required parameters to calculate a RA value using Kuzmin and Michailov's formulation,[51] film thickness, d, is obtained by taking into account the tilt angle for a molecule of known length; directional refractive indices of the film, n_x and n_z, are set to about 1.5; directional absorption coefficients of the film, k_x and k_z, are obtained for the given tilt angle and transition moment direction when the film absorption coefficient, k_{max}, is known.

It was pointed out that the reflectivity of film-free water surface for s polarization, R_s, was larger than that for p polarization, R_p, when the incident angle is close to Brewster angle.[32h,53] As a result, a small portion of s-polarized radiation "leaking" through the polarizer will lead to larger reflectivities from the film-free surfaces. So the observed RA will be smaller than the predicted one for pure p-polarized radiation. In contrast, RA for s-polarized radiation is practically undisturbed by p-polarized radiation leaking through the polarizer. The degree of polarization of the optical setup, Γ, should be taken into account to obtain effective reflectivities and real RA values. For a known polarizer, Γ is a constant value, which can be evaluated for a known tilt angle by comparing measured and calculated RA at a single incident angle for p and s polarization. In this experiment, the value of Γ is 0.013. Here only two unknowns remain, k_{max} and θ. We use a series of k_{max} values by computer simulation to calculate RA values to fit the measured RA values. The tilt angle θ should be obtained subsequently by the best fit. It is shown that a small change in k_{max} would give rise to a distinct difference in RA fit, particularly near Brewster angle, on the contrary, the tilt angle is less influenced.

Figures 8 and 9 show the theoretical RA of the s (dotted line) and p (solid line) polarization for the $\upsilon_a(CH_2)$ bands of the 1-(2-octadecyloxycarbonylethyl)cytosine monolayers on H_2O/D_2O (top) and H_2O/D_2O guanosine solution (bottom) subphases, respectively, against incident angle at various orientation angles

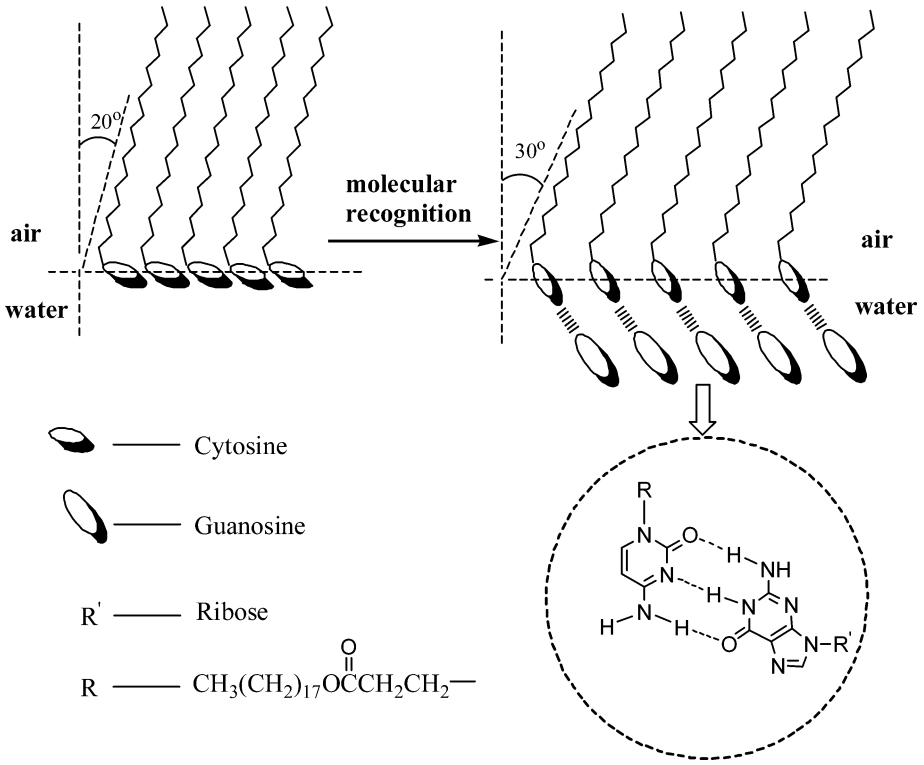

Figure 10. Schematic illustrations of molecular recognition between 1-(2-octadecyloxycarbonylethyl)cytosine monolayers and guanosine at the air−water interface along with the orientation of aromatic rings and alkyl chains prior to and after molecular recognition.

by using the obtained k_{max} value, 0.50. The black circles and squares represent the results obtained from the measurements for s and p polarization, respectively. In the case of p polarization, the theoretical RA intensity increases with incident angle and reaches a maximum value, while in the case of s polarization, the theoretical intensity decreases with incident angle. For the p polarization at the given incident angle, the theoretical RA intensity decreases with increasing tilt angle of molecular axis (chain axis). The measured values fit well with the theoretical curves for the tilt angle of the chains 20° with respect to the film normal before molecular recognition and 30° after molecular recognition both on the H_2O subphase and on the D_2O subphase. The theoretical calculation is consistent with the above qualitative deduction from the decrease of the band intensities. Schematic illustrations of molecular recognition between 1-(2-octadecyloxycarbonylethyl)cytosine monolayers at the air−water interface and guanosine in the subphase along with the orientation of cytosine rings and alkyl chains prior to and after molecular recognition are shown in Figure 10. The results indicate that the orientation of the alkyl chains is strongly influenced by the interaction between the headgroups in the monolayers and the complementary guanosine bases in the subphase. An increase in tilt angle of the alkyl chains in the monolayers from 20° before molecular recognition to 30° after molecular recognition should increase the fluidity of the nucleolipid monolayers, which is necessary for the functions of the nucleolipid monolayers.

Conclusions

The direct spectroscopic evidence for the molecular recognition of cytosine−guanosine base pairs at the air−water interface by means of triple hydrogen bonds in the exact sites of the cytosine rings is observed using IRRAS technique. The reduction in intensities of vibrational bands of the cytosine rings suggests that the cytosine rings undergo a flat-on orientation before molecular recognition to an end-on one after molecular recognition. The decrease in $\upsilon_a(CH_2)$ and $\upsilon_s(CH_2)$ intensities indicates that the alkyl chains are more tilted after molecular recognition. Theoretical simulation of the RA values of the $\upsilon_a(CH_2)$ modes to the measurement shows that the tilt angle of the alkyl chains undergoes a change from 20° before molecular recognition to 30° after molecular recognition both on the H_2O subphase and on the D_2O subphase, which suggests that the chain orientation is strongly influenced by the interaction between headgroups in the monolayers and the complementary guanosine bases in the subphase.

Acknowledgment. This work was financially supported by the National Natural Science Foundation of China (NSFC, No. 20273029).

References and Notes

(1) Lehn, J. M. *Supramolecular Chemistry*; VCH: Weinheim, 1995.
(2) Ringsdorf, H.; Schlarb, B.; Venzmer, J. *Angew. Chem., Int. Ed. Engl.* **1988**, *27*, 113.
(3) Piantadosi, C.; Marasco, C. J.; Morris-Natschke, S. L.; Meyer, K. L.; Gumus, F.; Surles, J. R.; Ishaq, K. S. *J. Med. Chem.* **1991**, *34*, 1408.
(4) Kimizuka, N.; Kawasaki, T.; Hirata, K.; Kunitake, T. *J. Am. Chem. Soc.* **1995**, *17*, 6360.
(5) Saenger, W. *Principles of Nucleic Acid Structure*; Springer-Verlag: New York, 1984; Chapter 6.
(6) Ts'o, P. O. P. In *Basic Principles in Nucleic Acid Chemistry*; Ts'o, P. O. P., Ed.; Academic Press: New York, 1974; Chapter 6.
(7) Cantor, C. R.; Shimmel, P. R. *Biophysical Chemistry*; W. H. Freeman and Co.: San Francisco, 1980; Parts I and II, Chapters 6 and 7.
(8) Nowick, J. S.; Chen, J. S.; Noronha, G. *J. Am. Chem. Soc.* **1993**, *115*, 7636.
(9) Nowick, J. S.; Cao, T.; Noronha, G. *J. Am. Chem. Soc.* **1994**, *116*, 3285.
(10) Berti, D.; Barbaro, P.; Bucci, H.; Baglioni, P. *J. Phys. Chem. B* **1999**, *103*, 4916.
(11) Onda, M.; Yoshihara, K.; Koyano, H.; Ariga, K.; Kunitake, T. *J. Am. Chem. Soc.* **1996**, *118*, 8524.

(12) Berti, D.; Barbaro, P.; Bonaccio, S.; Barsacchi-Bo, G.; Luisi, P. L. *J. Phys. Chem. B* **1998**, *102*, 303.
(13) Kimizuka, N.; Kawasaki, T.; Hirata, K.; Kunitake, T. *J. Am. Chem. Soc.* **1998**, *120*, 4094.
(14) Alhers, M.; Ringsdorf, H.; Rosemeyer, H.; Seela, F. *Colloid Polym. Sci.* **1990**, *268*, 132.
(15) Kurihara, K.; Ohto, K.; Honda, Y.; Kunitake, T. *J. Am. Chem. Soc.* **1991**, *113*, 5077.
(16) Berndt, P.; Kurihara, K.; Kunitake, T. *Langmuir* **1995**, *11*, 3083.
(17) Berti, D.; Franchi, L.; Baglioni, P. *Langmuir* **1997**, *13*, 3438.
(18) Shimomura, H.; Nakamura, F.; Ijiro, K.; Taketsuna, H.; Tanaka, M.; Nakamura, H.; Hasbe, K. *J. Am. Chem. Soc.* **1997**, *119*, 2341.
(19) Räler, U.; Heiz, C.; Luisi, P. L.; Tampé, R. *Langmuir* **1998**, *14*, 6620.
(20) Weck, M.; Fink, R.; Ringsdorf, H. *Langmuir* **1997**, *13*, 3515.
(21) Ding, D.; Zhang, Z.; Shi, B.; Luo, X.; Liang, Y. *Colloids Surf.* **1996**, *112*, 25.
(22) Huang, J.; Liang, Y. *Thin Solid Films* **1998**, *326*, 217.
(23) Huang, J.; Liang, Y. *Thin Solid Films* **1998**, *325*, 210.
(24) Huang, J.; Li, C.; Liang, Y. *Langmuir* **2000**, *16*, 3937.
(25) Li, C.; Huang, J.; Liang, Y. *Langmuir* **2000**, *16*, 7701.
(26) Li, C.; Huang, J.; Liang, Y. *Langmuir* **2001**, *17*, 2228.
(27) Miao, W.; Du, X.; Liang, Y. *Langmuir* **2003**, *19*, 5389.
(28) Huo, Q.; Dziri, L.; Desbat, B.; Russell, K. C.; Leblanc, R. M. *J. Phys. Chem. B* **1999**, *103*, 2929.
(29) Kitano, H.; Ringsdorf, H. *Bull. Chem. Soc. Jpn.* **1985**, *58*, 2826.
(30) (a) Blaudez, D.; Buffeteau, T.; Cornut, J. C.; Desbat, B.; Excafre, N.; Pezolet, M.; Turlet, J. M. *Appl. Spectrosc.* **1993**, *47*, 869. (b) Blaudez, D.; Turlet, J. M.; Dufourcq, J.; Bard, D.; Buffeteau, T.; Desbat, B. *J. Chem. Soc., Faraday Trans.* **1996**, *92*, 525.
(31) Sakai, H.; Umemua, J. *Chem. Lett.* **1993**, 2167.
(32) (a) Flach, C. R.; Braunder, J. W.; Taylor, J. W.; Baldwin, R. C.; Mendelsohn, R. *Biophys. J.* **1994**, *67*, 402. (b) Flach, C. R.; Braunder, J. W.; Mendelsohn, R. *Appl. Spectrosc.* **1993**, *47*, 982. (c) Pastrana-Rios, B.; Flach, C. R.; Braunder, J. W.; Mautone, A. J.; Mendelsohn, R. *Biophys. J.* **1993**, *65*, 1994. (d) Flach, C. R.; Mendelsohn, R. *Biophys. J.* **1993**, *64*, 1113. (e) Flach, C. R.; Prendergast, F. G.; Mendelsohn, R. *Biophys. J.* **1996**, *70*, 539. (f) Mendelsohn, R.; Braunder, J. W.; Gericke, A. *Annu. Rev. Phys. Chem.* **1995**, *46*, 305. (g) Gericke, A.; Mendelsohn, R. *Langmuir* **1996**, *12*, 758. (h) Flach, C. R.; Gericke, A.; Mendelsohn, R. *J. Phys. Chem. B* **1997**, *101*, 58. (i) Gericke, A.; Flach, C. R.; Mendelsohn, R. *Biophys. J.* **1997**, *73*, 492. (j) Wu, F. J.; Gericke, A.; Flach, C. R.; Mealy, T. R.; Seaton, B. A.; Mendelsohn, R. *Biophys. J.* **1998**, *74*, 3273. (k) Dieudonne, D.; Gericke, A.; Flach, C. R.; Jiang, X.; Farid, R.; Mendelsohn, R. *J. Am. Chem. Soc.* **1998**, *120*, 792. (l) Wu, F. J.; Flach, C. R.; Seaton, B. A.; Mealy, T. R.; Mendelsohn, R. *Biochemistry* **1999**, *38*, 792.
(33) (a) Riou, S. A.; Hsu, S. L.; Stidham, H. D. *Langmuir* **1998**, *14*, 3062. (b) Riou, S. A.; Hsu, S. L.; Stidham, H. D. *Biophys. J.* **1999**, *75*, 2451. (c) Chen, H.; Hsu, S. L.; Tirrell, D. A.; Stidham, H. D. *Langmuir* **1997**, *13*, 4775.
(34) Ohe, C.; Ando, H.; Sato, N.; Urai, Y.; Yamamoto, M.; Itoh, K. *J. Phys. Chem. B* **1999**, *103*, 435.
(35) Reitzel, N.; Greve, D. R.; Kjaer, K.; Howes, P. B.; Jayaraman, M.; Savoy, S.; McCullough, R. D.; McDevitt, J. T.; Bjornholm, T. *J. Am. Chem. Soc.* **2000**, *122*, 5788.
(36) Ren, Y.; Iimura, K.; Kato, T. *Langmuir* **2001**, *17*, 2688.
(37) Chernyshova, I. V.; Rao, K. H. *J. Phys. Chem. B* **2001**, *105*, 810.
(38) Schmitt, L.; Bohanon, T. M.; Denzinger, S.; Ringsdorf, H.; Tampe, R. *Angew. Chem., Int. Ed. Engl.* **1996**, *35*, 317.
(39) (a) Gericke, A.; Simmon-Kustscher, J.; Hühnerfuss, H. *Langmuir* **1993**, *9*, 2119. (b) Gericke, A.; Simmon-Kustscher, J.; Hühnerfuss, H. *Langmuir* **1993**, *9*, 3115. (c) Gericke, A.; Hühnerfuss, H. *J. Phys. Chem.* **1993**, *97*, 12899. (d) Gericke, A.; Hühnerfuss, H. *Thin Solid Films* **1994**, *245*, 72. (e) Gericke, A.; Hühnerfuss, H. *Ber. Bunsen-Ges. Phys. Chem.* **1995**, *99*, 641. (f) Gericke, A.; Hühnerfuss, H. *Langmuir* **1995**, *11*, 225. (g) Neumann, V.; Gericke, A.; Hühnerfuss, H. *Langmuir* **1995**, *11*, 2206. (h) Simmon-Kustscher, J.; Gericke, A.; Hühnerfuss, H. *Langmuir* **1996**, *12*, 1027. (i) Gericke, A.; Hühnerfuss, H. *Chem. Phys. Lett.* **1994**, *74*, 205. (j) Hühnerfuss, H.; Neumann, V.; Stine, K. J. *Langmuir* **1996**, *12*, 2561. (k) Hoffmann, F.; Hühnerfuss, H.; Stine, K. J. *Langmuir* **1998**, *14*, 4525. (l) Overs, M.; Hoffmann, F.; Schäfer, H. J.; Hühnerfuss, H. *Langmuir* **2000**, *16*, 6995.
(40) Fina, L. J.; Tung, Y. *Appl. Spectrosc.* **1991**, *45*, 986.
(41) Adnet, F.; Liquier, J.; Taillandier, E.; Singh, M. P.; Rao, K. H.; Lown, J. W. *J. Biol. Struct.* **1992**, *10*, 565.
(42) (a) Dluhy, R. A.; Cornell, D. G. *J. Phys. Chem.* **1985**, *89*, 3195. (b) Dluhy, R. A. *J. Phys. Chem.* **1986**, *90*, 1373. (c) Mitchell, M. L.; Dluhy, R. A. *J. Am. Chem. Soc.* **1988**, *110*, 712. (d) Dluhy, R. A.; Wright, N. A.; Griffiths, P. R. *Appl. Spectrosc.* **1988**, *42*, 138. (e) Dluhy, R. A.; Mendelsohn, R. *Anal. Chem.* **1988**, *60*, 269.
(43) Sapper, H.; Cameron, D. G.; Mantsch, H. H. *Can. J. Chem.* **1981**, *59*, 2543.
(44) Cameron, D. G.; Martin, A.; Moffatt, D. J.; Mantsch, H. H. *Biochemistry* **1985**, *24*, 4355.
(45) Tian, Y. *J. Phys. Chem.* **1991**, *95*, 9985.
(46) Aamouche, A.; Ghomi, M.; Grajcar, L.; Baron, M. H.; Romain, F.; Baumruk, V.; Stepanek, J.; Coulombeau, C.; Jobic, H.; Berthier, G. *J. Phys. Chem. A* **1996**, *100*, 5578.
(47) Lord, R. C.; Thomas, G. J., Jr. *Spectrochim. Acta* **1967**, *23A*, 2551.
(48) Szczepaniak, K.; Szczepaniak, M. *J. Mol. Struct.* **1987**, *156*, 29.
(49) Du, X.; Shi, B.; Liang, Y. *Langmuir* **1998**, *14*, 3631.
(50) Schopper, H. *Z. Phys.* **1952**, *132*, 146.
(51) (a) Kuzmin, V. L.; Michailov, A. V. *Opt. Spectrosc.* **1981**, *51*, 383. (b) Kuzmin, V. L.; Romanov, V. P.; Michailov, A. V. *Opt. Spectrosc.* **1992**, *73*, 3.
(52) Yamamato, K.; Ishida, H. *Appl. Spectrosc.* **1994**, *48*, 775.
(53) Gericke, A.; Michailov, A. V.; Hühnerfuss, H. *Vib. Spectrosc.* **1993**, *4*, 335.
(54) Tung, Y.; Gao, T.; Rosen, M. J.; Valentini, J. E.; Fina, L. J. *Appl. Spectrosc.* **1993**, *47*, 1643.
(55) Ren, Y.; Meuse, C. W.; Hsu, S. L.; Stidham, H. D. *J. Phys. Chem.* **1994**, *98*, 8424.
(56) Bertie, J. E.; Ahmed, M. K.; Eysel, H. H. *J. Phys. Chem.* **1989**, *93*, 2210.